A MULTI-FRAME OPTICAL FLOW SPOT TRACKER

Jizhou Li, Christopher Gilliam, and Thierry Blu

Department of Electronic Engineering, The Chinese University of Hong Kong
Email: {jzli, cgilliam, tblu}@ee.cuhk.edu.hk.

ABSTRACT

Accurate and robust spot tracking is a necessary tool for quantitative motion analysis in fluorescence microscopy images. Few trackers however consider the underlying dynamics present in biological systems. For example, the collective motion of cells often exhibits both fast dynamics, i.e. Brownian motion, and slow dynamics, i.e. time-invariant stationary motion. In this paper, we propose a novel, multi-frame, tracker that exploits this stationary motion. More precisely, we first estimate the stationary motion and then use it to guide the spot tracker. We obtain the stationary motion by adapting a recent optical flow algorithm that relates one image to another locally using an all-pass filter. We perform this operation over all the image frames simultaneously and estimate a single, stationary optical flow. We compare the proposed tracker with two existing techniques and show that our approach is more robust to high noise and varying structure. In addition, we also show initial experiments on real microscopy images.

Index Terms— Spot tracking, stationary motion, fluorescence microscopy, optical flow, all-pass filters

1. INTRODUCTION

Recent developments in fluorescence microscopy, such as improved optics, electronic imaging and new fluorescent probes [1, 2], have enabled biologists to observe and investigate biological systems, such as intracellular processes, at an unprecedented spatiotemporal resolution [3]. A major challenge, therefore, is to understand not just the spatial organization of biological systems but their spatiotemporal relationship [4]. A key technique used in the analysis of this relationship is spot tracking [3] - following the position of a spot over a series of time frames. However, robust and accurate tracking is difficult due to high noise levels in microscopy images [2] and fast dynamics, such as Brownian motion [5].

Numerous spot tracking methods have been proposed for different biological applications, for example see [6, 7, 8, 9] to list but a few. In general, these tracking methods all follow the same procedure: preprocess the image data, detect the spots in each frame and then link the detected spots over time to create trajectories [2]. A survey of spot detection in fluorescence microscopy was presented in [5], however, a recent evaluation of spot trackers, designed for microscopy imaging, found no one method outperformed the others in all situations [3]. The more general problem of object tracking has also been extensively studied in image processing. A particularly popular method, used in applications such as crowd analysis [10, 11], is the Kanade-Lucas-Tomasi (KLT) tracker proposed in [12]. The KLT Tracker is based on Lucas and Kanade's optical

flow algorithm [13]. For a comprehensive review of the state-of-the-art see [14, 15].

In this paper, unlike existing approaches in the spot tracking literature [3, 6, 7], we propose a multi-frame optical flow tracker that exploits global motion characteristics present in biological systems. More precisely, we assume there exists a motion pattern that underpins the dynamics within the system being imaged. We define this underlying motion as the main part of the motion between any two consecutive images in the sequence that does not change, i.e. the *stationary motion field*. This type of stationary motion has been observed in many organisms, such as crowds of people [16], flocks of birds [17] and bacteria [18]. In particular, in the study of the collective motion behavior of cells, the structural movement often exhibits stable flow dynamics which do not significantly change over the period of several frames [19]. Hence, we propose to improve accuracy and robustness by using this stationary motion to guide the spot tracking.

Similar to [12], we use an optical flow algorithm to estimate the stationary motion. Instead of enforcing temporal coherence on a frame-by-frame basis [20], we estimate a single optical flow for the whole image sequence using an adapted version of the algorithm proposed in [21]. This algorithm consists of relating local changes in one image to another image using all-pass filters and then extracting the optical flow from the filters. Our approach is to perform this operation over all the image frames simultaneously. We compare the proposed method with two existing tracking techniques for synthetic image sequences, which mimic the images obtained from confocal microscopy. We also demonstrate the applicability of the method for the estimation and tracking of multiple spot movements in real fluorescence confocal microscopy images.

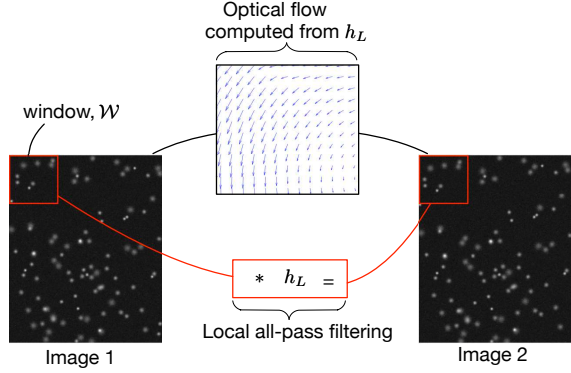## 2. OPTICAL FLOW ESTIMATION USING LOCAL ALL-PASS FILTERS

Recently, Gilliam and Blu [21] presented a novel algorithm for optical flow estimation; termed the Local All-Pass (LAP) algorithm. Instead of using the optical flow equation [13, 22], the authors estimate the flow using local all-pass filters. In this paper, we want to adapt the LAP to estimate a stationary motion field. Accordingly, before proceeding, we outline the main aspects of the algorithm.

2.1. Idea 1 - Shifting is all-pass filtering

The central concept of the LAP algorithm is that a constant optical flow is equivalent to filtering with an all-pass filter. To observe this equivalence, consider two images, I_1 and I_2, relate by a constant optical flow, $u = [u_x, u_y]^T$. Assuming brightness consistency [23], the two images can be related as $I_2(x, y) = I_1(x - u_x, y - u_y)$, where (x, y) is the pixel coordinates. In the Frequency domain, this

Fig. 1. Diagram illustrating optical flow estimation using the Local All-Pass (LAP) algorithm. The LAP assumes the optical flow is locally constant in a window $\mathcal{W}$ and that this local flow is equivalent to a convolution with a local all-pass filter h_L. Moving the window results in a new local filter. The flow is then extracted from the local all-pass filters.

relation is equivalent to:

$$\hat{I}_2(e^{jw_x}, e^{jw_y}) = \hat{I}_1(e^{jw_x}, e^{jw_y}) e^{-ju_x\omega_x - ju_y\omega_y}, \quad (1)$$

where $\hat{I}$ represents the 2D discrete time Fourier transform of the images and (w_1, w_2) denotes the 2D frequency coordinates. Now, if we define $H(e^{jw_x}, e^{jw_y}) = e^{-ju_x w_x - ju_y w_y}$, then I_2 is a filtered version of I_1 and the filter, H, is all-pass in nature.

2.2. Idea 2 - FIR approximation of the all-pass filter

Importantly, the frequency response of the all-pass filter H can always be expressed as

$$H(e^{jw_x}, e^{jw_y}) = \frac{P(e^{jw_x}, e^{jw_y})}{P(e^{-jw_x}, e^{-jw_y})}, \quad (2)$$

where $P(e^{jw_x}, e^{jw_y})$ is the forward and $P(e^{-jw_x}, e^{-jw_y})$ is the backward version of a filter P respectively. Given this structure, [21] approximate the all-pass filtering using a forward-backward FIR filtering scheme that involves P. In other words, in the pixel domain, we now have the following filtering relationship

$$p(-x, -y) * I_2(x, y) = p(x, y) * I_1(x, y), \quad (3)$$

where $*$ denotes convolution. Therefore, estimating the FIR filter P is equivalent to estimating the all-pass filter H.

2.3. Idea 3 - A basis representation of the FIR filtering

The final element in the LAP algorithm is to approximate the FIR filter P as a linear combination of a few filters, $P_n(e^{jw_1}, e^{jw_2})$, i.e. a basis representation:

$$P(z_1, z_2) = \sum_{n=0}^{N-1} c_n P_n(z_1, z_2), \quad (4)$$

where N is some small number (either 3 or 6) and c_n are the coefficients. As a consequence, determining the all-pass filter H amounts to estimating the coefficients $\{c_n\}_{n=0,\dots,N-1}$ assuming the forward-backward filtering scheme in (3). The basis in question

comprised a family of filters based on the Gaussian function and its derivatives. For this paper, we shall restrict the basis to the first three elements, i.e. $N = 3$. Therefore, the filter basis is

$$p_0(x, y) = e^{-\frac{x^2+y^2}{2\sigma^2}},$$
$$p_1(x, y) = xp_0(x, y) \quad \text{and} \quad p_2(x, y) = yp_0(x, y), \quad (5)$$

where $\sigma = (W + 2)/4$. The advantage of these filters is that they are completely scalable and are typically suited for flows of displacement up to W pixels.

2.4. Local All-Pass (LAP) Algorithm

Now, using the above ideas, the LAP algorithm functions by assuming the optical flow is constant within a local window $\mathcal{W}$ and estimating an all-pass filter, for that window, using (3) and (4). Once this local filter is obtained, the window $\mathcal{W}$ is shifted and a new all-pass filter is estimated. The result is that a local all-pass filter is estimated per pixel (a filter corresponds to the central pixel in $\mathcal{W}$). A diagram illustrating the LAP is shown in Fig. 1. The exact minimization solved at each pixel is

$$\min_{\{c_n\}} \sum_{x,y \in \mathcal{W}} |p(-x, -y) * I_2(x, y) - p(x, y) * I_1(x, y)|^2, \quad (6)$$

where $p(x, y) = p_0(x, y) + \sum_{n=1}^{N-1} c_n p_n(x, y)$ and $\mathcal{W}$ is the local region with size $(2W + 1) \times (2W + 1)$. Importantly, this solution can be implemented very efficiently using convolution and pointwise multiplication [21].

The final stage of the LAP algorithm is to extract the optical flow estimates from the local all-pass filters. Based on the ideal response in (1), the following expressions were proposed involving the impulse response of the filter P:

$$u_x = 2\frac{\sum_{x,y} xp(x, y)}{\sum_{x,y} p(x, y)} \quad \text{and} \quad u_y = 2\frac{\sum_{x,y} yp(x, y)}{\sum_{x,y} p(x, y)}. \quad (7)$$

3. STATIONARY LOCAL ALL-PASS TRACKER

In this section, we present a novel spot tracker that uses time-invariant (i.e. stationary) motion information to help guide its tracking. The stationary motion is obtained by adapting the LAP algorithm, hence we call the tracker the Stationary Local All-Pass (SLAP) Tracker. The tracker consists of three stages: i) estimation of an underlying stationary motion field; ii) simple spot detection; iii) trajectory estimation based on the stationary motion field. We now expand upon these stages.

3.1. Stationary Motion Estimation using Local All-Pass Filters

Collective behavior has been observed in many organisms, such as plant cells [19], birds [17], bacteria [18] and crowds [11]. The central assumption behind it is that there exists an underlying motion pattern that is stationary over the image sequence. A similar idea, termed the *floor field*, was proposed in [16] for optical flow estimation in crowd analysis. This floor field was obtained by estimating the optical flow between every pair of images in the sequence and then averaging across time. In contrast, we propose estimating one single optical flow, $\bar{u}(x, y)$, from the whole image sequence directly, i.e. a stationary motion field. To estimate this motion, we adapt the algorithm in Section 2 and hence obtain the stationary local all-pass (SLAP) algorithm.

(a) Spot Detection   (b) Trajectory Estimation
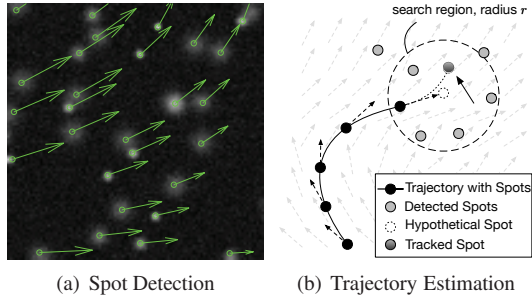
Fig. 2. Illustration of the SLAP Tracker. (a) The detected spots and extracted flow vectors from the SLAP algorithm; (b) Trajectory Estimation by linking spots across different image frames. The black circles and line indicate spots already joined into a trajectory. Dark gray circles indicate the detected spots in the next frame. Open circle represents the estimated spot position by the flow. The black arrow points out which one will be chosen to be added to the trajectory.

Specifically, our goal is to determine the stationary flow, $\bar{u}(x,y) = [\bar{u}_x(x,y), \bar{u}_y(x,y)]^{\mathrm{T}}$, from a given sequence of images $I(x,y,t), t = 0, 1, ..., T-1$, where T is the number of time frames. As a consequence, to handle multiple time frames simultaneously, we adapt the minimization in (6) to:

$$\min_{\{c_n\}} \sum_{t=0}^{T-1} \sum_{x,y \in \mathcal{W}} |p(-x,-y) * I_2(x,y,t) - p(x,y) * I_1(x,y,t)|^2,$$

where $\{c_n\}$ are the coefficients for the filter p. The stationary motion field is then obtained using the equations in (7).

3.2. Detection and Trajectory Estimation

Spots Detection: In image processing, there exists many methods to detect spots (or more general features), for example Gaussian fitting, using the Laplacian of Gaussian or detecting SIFT features [24]. For a complete review of the state-of-the-art see [5, 25]. In this paper, we opt for a low complexity detection method: the Gaussian mask correlation method proposed in [26]. We first remove small image values using a threshold, thus determining regions that many contain spots. Given these regions, we then compute their correlation with a pre-defined Gaussian mask. Finally, the spot locations are estimated by finding the local maxima of the correlations. Note that we obtain a motion vector for each spot from the flow estimated using the SLAP algorithm. A typical example is shown in Fig. 2(a).

Trajectory Estimation: Let X_i stands for the position of a spot g_i in frame i, using the stationary motion field, $\bar{u}$, the motion vector for this spot is $v_i = \bar{u}(X_i)$. Accordingly, in ideal conditions, the position of the spot in frame $i+1$, i.e. g_{i+1}, should be $\hat{X}_{i+1} = X_i + v_i$. However, due to model mis-match, this many not be the case. As a consequence, we use $\hat{X}_{i+1}$ as the center of a circular search region, of radius r, in which we aim to find g_{i+1}. More precisely, within the search region, we have a set of candidate spots. From these candidates, we choose the closest spot to $\hat{X}_{i+1}$ based on the Euclidean distance. The chosen spot is then labeled g_{i+1} and X_{i+1} is set to its position. Finally, this procedure is repeated for all frames thus constructing a trajectory for the spot. The end result of the SLAP tracker will be a set of trajectories relating to the spots detected. An illustration of this trajectory estimation is shown in Fig. 2(b).

(a) Correct   (b) Incorrect
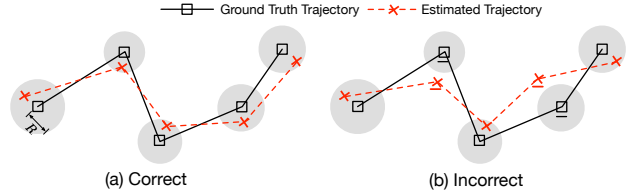
Fig. 3. Illustration of trajectory evaluation. Diagram (a) shows a correctly estimated trajectory and (b) shows an incorrect trajectory. A trajectory is correct if all its estimated positions (crosses) fall within a certain radius, R, of the ground truth positions (squares). The positions that fail this criteria are marked as underscored crosses.

(a) Dynamic Models   (c) Image Quality
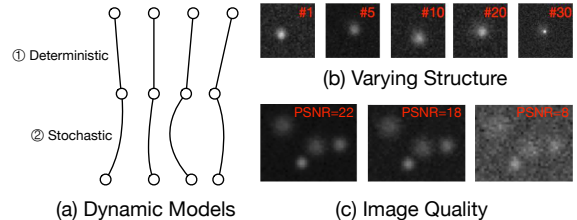
Fig. 4. Examples of the different variations allowed in the synthetic model. (a) The trajectories of two different motion models, Deterministic and Stochastic respectively. (b) Intensity profiles of generated spots with varying structures over different frames. (c) Image quality for generated spots with different levels of noise.

4. EXPERIMENT AND RESULTS

4.1. Performance Evaluation

The result of a spot tracking algorithm is a series of trajectories that detail the position of each tracked spot at each time point. Given these estimated trajectories and access to the ground-truth, we evaluate the performance of a tracker using a conservative measure; either a trajectory is correctly identified or it is not. Our definition of a correctly identified trajectory is: for each time point in the trajectory, the estimated position of the spot is within a certain radius, R, of the actual spot's position. A diagram illustrating this concept is shown in Fig. 3. Accordingly, we can evaluate a tracker based upon the percentage of correctly identified trajectories. The advantage of this approach is that it provides a straightforward, intuitive, measure of a tracker's overall ability to track spots.
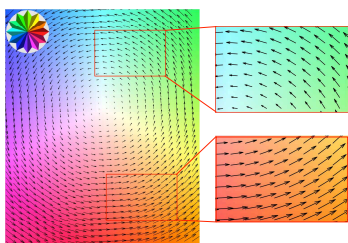
4.2. Synthetic Images

Simulation Setup: The synthetic image sequence consists of two elements: the spots we wish to track and the underlying stationary motion that controls their movement. To mimic the images obtained from a confocal microscopy, similar to [3], we choose to model the spots using an isotropic 2D Gaussian function; the variance, σ_g, of the function dictates the size of the spot and its amplitude. Note that we set $R = 2\sqrt{2\ln(2)}\sigma_g$ when evaluating the trajectory. In these simulations, we generate 100 spots that are randomly positioned in a 245×200 pixel image. Having defined the spots, we then model their movement over 30 time frames using the Lamb-Oseen vortex model [27]. This model generates a spiral stationary motion field that is illustrated in Fig. 5. Note that the maximum displacement of the motion, at one time instance, is 8 pixels.

In practice, however, biological systems observed via microscopy are subject to noise. We therefore introduce three types

Scenarios	KLT Tracker			Particle Tracker			SLAP Tracker		
	PSNR=22	PSNR=18	PSNR=8	PSNR=22	PSNR=18	PSNR=8	PSNR=22	PSNR=18	PSNR=8
Deterministic+Constant	56%	56%	53%	75%	74%	57%	**90%**	**87%**	**76%**
Deterministic+Varying	51%	54%	47%	67%	63%	48%	**80%**	**75%**	**62%**
Stochastic+Constant	29%	28%	23%	39%	38%	31%	**62%**	**60%**	**50%**
Stochastic+Varying	27%	24%	18%	38%	29%	23%	**59%**	**57%**	**45%**

Table 1. Comparison results of the tracking algorithms when applied to synthetic images in different scenarios. The algorithms are compared in terms of the percentage of correctly identified trajectories (there are 100 spots to track in total). *Constant/Varying* represents the profile of the spot structure and *Deterministic/Stochastic* represents the dynamic model. The bold values indicate the best results.
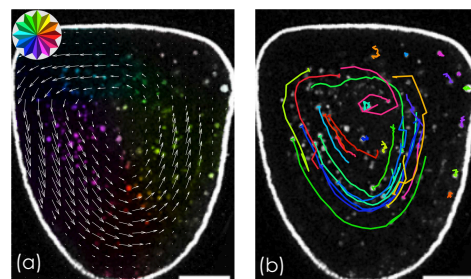

Fig. 5. A visualization of the underlying motion field used in the synthetic image sequence. Note that the direction and magnitude of the motion is color coded (the key is in the top left).

Fig. 6. SLAP Tracker results for real microscopy images. (a) The estimated stationary motion field obtained from the SLAP algorithm. Note that the direction is color coded (*top left*). (b) The trajectories of 32 spots built by the Tracker.

of noise corruption. The first is to corrupt the final images using additive Gaussian noise, see Fig. 4(c). The peak-signal-to-noise-ratio (PSNR) of the noise is either 8dB, 18dB or 22dB. The second corruption is to allow the structure and intensity of the spots to slowly vary over time (i.e allow the variance of the Gaussian functions to change). An example of the time varying structure is shown in Fig. 4(b). Finally, the third corruption is to add a stochastic variation to the motion field at each time instance. In other words, the movement of the spots is modeled as a deterministic element, due to the stationary motion, plus a stochastic element (e.g. Brownian motion), see Fig. 4(a). Given these options, we examine four different scenarios: (i) deterministic motion and constant spot structure; (ii) deterministic motion but time varying spot structure; (iii) deterministic+stochastic motion but constant spot structure; (iv) deterministic+stochastic motion and time varying spot structure. Note that, in all scenarios, we corrupt the images using the additive Gaussian noise defined above.

Tracking results: We compare the SLAP Tracker with two existing tracking techniques: KLT Tracker [12], which is based on the Lucas-Kanade optical flow algorithm [13], and Particle Tracker [6], which is one of the state-of-the-art methods identified in [3]. We use the implementation of the KLT Tracker available at http://www.ces.clemson.edu/%7estb/klt/ and the ImageJ plug-in of the Particle Tracker.

The results, see Tab. 1, show that our SLAP Tracker outperforms the other two algorithms in all conditions. In particular, when the spots have a constant structure and deterministic trajectories, scenario (i), the SLAP Tracker achieves an average accuracy of 84.3% across all noise levels. For the most challenging, scenario (iv), this average accuracy drops to 53.7% however the equivalent accuracy for the Particle Tracker and the KLT Tracker is 30.0% and 23.0%, respectively. Accordingly, the results demonstrate the advantage of using the optical flow estimated from the SLAP algorithm for accurate spot tracking. In terms of computational complexity, the main cost in the SLAP Tracker occurs when calculating the stationary motion field; the simple detection and linking strategies employed have low computational cost. However, although a per

pixel motion field may seem costly, it is only calculated once across all the images using a very fast algorithm [21], thus it is independent of the spot number. In contrast, the KLT Tracker is required to estimate the optical flow locally for each spot in every image. Movies illustrating the performance and results can be found online at http://www.ee.cuhk.edu.hk/%7ejzli/SLAPTracker.

4.3. Real Images

In this section, we demonstrated the proposed SLAP Tracker on a real image sequence. The sequence depicts cytoplasmic streaming in Drosophila oocytes (fruit fly eggs) and is obtained from [28]. Drosophila oocytes provide a good system to investigate microtubule-dependent transport, and microtubule motors are important both for targeted localization of polarity determinant mRNAs. The stationary motion field obtained by the SLAP algorithm is shown in Fig. 6 (a); it explicitly reveals the underlying motion behind the cytoplasmic streaming. The results of tracking 32 spots are shown in Fig. 6 (b). We observed that the SLAP Tracker successfully followed 25 spots (correctness=83.3%) during 30 consequent frames until their disappearance.

5. CONCLUSIONS

We have presented a novel multi-frame optical flow-based approach, SLAP Tracker, for spot tracking in image sequences. The approach is based estimating the underlying, stationary, motion of the biological system and using it to guide the tracking of spots. This stationary motion field is estimated from all the images simultaneously using local all-pass filters. We validated the accuracy of the SLAP Tracker using synthetic images with complicated motion patterns, intensity variation and high noise, and it was shown to outperform two existing approaches in terms of correct trajectory estimation. We then demonstrated the potential applicability of the SLAP Tracker for real biological applications.

6. REFERENCES

[1] C. Vonesch, F. Aguet, J.-L. Vonesch, and M. Unser, "The colored revolution of bioimaging," *IEEE Signal Process. Mag.*, vol. 23, no. 3, pp. 20–31, 2006.

[2] E. Meijering, I. Smal, and G. Danuser, "Tracking in molecular bioimaging," *IEEE Signal Process. Mag.*, vol. 23, no. 3, pp. 46–53, 2006.

[3] N. Chenouard *et al.*, "Objective comparison of particle tracking methods," *Nat. Methods*, vol. 11, no. 3, pp. 281–289, 2014.

[4] E. Meijering, I. Smal, O. Dzyubachyk, and J.-C. Olivo-Marin, "Chapter 15 - time-lapse imaging," in *Microscope Image Processing*, Q. Wu, F. Merchant, and K. Castleman, Eds., pp. 401 – 440. Academic Press, 2008.

[5] I. Smal, M. Loog, W. Niessen, and E. Meijering, "Quantitative comparison of spot detection methods in fluorescence microscopy," *IEEE Trans. Med. Imag.*, vol. 29, no. 2, pp. 282–301, 2010.

[6] I. Sbalzarini and P. Koumoutsakos, "Feature point tracking and trajectory analysis for video imaging in cell biology," *J. Struct. Biol.*, vol. 151, no. 2, pp. 182–195, 2005.

[7] I. Smal, K. Draegestein, N. Galjart, W. Niessen, and E. Meijering, "Particle filtering for multiple object tracking in dynamic fluorescence microscopy images: Application to microtubule growth analysis," *IEEE Trans. Med. Imag.*, vol. 27, no. 6, pp. 789–804, 2008.

[8] W. Godinez Navarro and K. Rohr, "Tracking multiple particles in fluorescence time-lapse microscopy images via probabilistic data association," *IEEE Trans. Med. Imag.*, 2014, preprint, doi: 10.1109/TMI.2014.2359541.

[9] L. Liang, S. Hongying, P. De Camilli, and J. Duncan, "A novel multiple hypothesis based particle tracking method for clathrin mediated endocytosis analysis using fluorescence microscopy.," *IEEE Trans. Image Process.*, vol. 23, no. 4, pp. 1844–1857, 2014.

[10] J. Jacques Junior, S. Raupp Musse, and C. Jung, "Crowd analysis using computer vision techniques," *IEEE Sig. Process. Mag.*, vol. 27, no. 5, pp. 66–77, 2010.

[11] T. Li, H. Chang, M. Wang, B. Ni, R. Hong, and S. Yan, "Crowded scene analysis: A survey," *IEEE Trans. Circuits Syst. Video Technol.*, 2015, preprint, doi: 10.1109/TCSVT.2014.2358029.

[12] J. Shi and C. Tomasi, "Good features to track," in *Proc. Computer Vision and Pattern Recognition (CVPR)*, Seattle, Washington, June 1994, pp. 593–600.

[13] B. D. Lucas and T. Kanade, "An iterative image registration technique with an application to stereo vision.," in *Proc. Int. Joint Conf. Artificial Intell.*, Vancouver, Canada, 1981, vol. 81, pp. 674–679.

[14] A. Yilmaz, O. Javed, and M. Shah, "Object tracking: A survey," *ACM computing surveys (CSUR)*, vol. 38, no. 4, pp. 13, 2006.

[15] K. Mikolajczyk and C. Schmid, "A performance evaluation of local descriptors," *IEEE Trans. Pattern Anal. and Mach. Intell.*, vol. 27, no. 10, pp. 1615–1630, 2005.

[16] S. Ali and M. Shah, "Floor fields for tracking in high density crowd scenes," in *Proc. European Conf. Comput. Vision (ECCV)*, pp. 1–14. Marseille, France, Oct. 2008.

[17] M. Ballerini *et al.*, "Interaction ruling animal collective behavior depends on topological rather than metric distance: Evidence from a field study," *Proc. Natl. Acad. Sci.*, vol. 105, no. 4, pp. 1232–1237, 2008.

[18] E. B. Jacob, Y. Aharonov, and Y. Shapira, "Bacteria harnessing complexity," *Biofilms*, vol. 1, no. 04, pp. 239–263, 2004.

[19] F. G. Woodhouse and R. E. Goldstein, "Cytoplasmic streaming in plant cells emerges naturally by microfilament self-organization," *Proc. Natl. Acad. Sci.*, vol. 110, no. 35, pp. 14132–14137, 2013.

[20] S. Volz, A. Bruhn, L. Valgaerts, and H. Zimmer, "Modeling temporal coherence for optical flow," in *Proc. IEEE Int. Conf. Comput. Vision (ICCV)*, Barcelona, Spain, 2011, pp. 1116–1123.

[21] C. Gilliam and T. Blu, "Local all-pass filters for optical flow estimation," in *Proc. IEEE Int. Conf. Acoust Speech Signal Process. (ICASSP)*, Brisbane, Australia, April 2015, accepted, http://www.ee.cuhk.edu.hk/%7etblu/publications/gilliam1501.pdf.

[22] B. K. Horn and B. G. Schunck, "Determining optical flow," *Artif. Intell.*, vol. 17, no. 1, pp. 185–203, 1981.

[23] S. Baker, D. Scharstein, J. Lewis, S. Roth, M. Black, and R. Szeliski, "A database and evaluation methodology for optical flow," *Int. J. Comput. Vis.*, vol. 92, no. 1, pp. 1–31, 2011.

[24] D. Lowe, "Distinctive image features from scale-invariant keypoints," *Int. J. Comput. Vis.*, vol. 60, no. 2, pp. 91–110, 2004.

[25] P. Ruusuvuori, T. Äijö, S. Chowdhury, C. Garmendia-Torres, J. Selinummi, M. Birbaumer, A. Dudley, L. Pelkmans, and O. Yli-Harja, "Evaluation of methods for detection of fluorescence labeled subcellular objects in microscope images," *BMC Bioinformatics*, vol. 11, no. 1, pp. 248, 2010.

[26] K. Takehara and T. Etoh, "A study on particle identification in PTV particle mask correlation method," *J. Vis.*, vol. 1, no. 3, pp. 313–323, 1999.

[27] W. Devenport, M. Rife, S. Liapis, and G. Follin, "The structure and development of a wing-tip vortex," *J. Fluid Mech.*, vol. 312, pp. 67–106, 1996.

[28] L. Serbus, B.-J. Cha, W. Theurkauf, and W. Saxton, "Dynein and the actin cytoskeleton control kinesin-driven cytoplasmic streaming in drosophila oocytes," *Development*, vol. 132, no. 16, pp. 3743–3752, 2005.